

Isolation, X-ray Structural Characterization, and Reactivities of Diiodosamarium(II) Complexes Bearing Amide Compounds as Ligands

Masayoshi Nishiura, Kosuke Katagiri, and Tsuneo Imamoto*

Department of Chemistry, Faculty of Science, Chiba University, Yayoi-cho, Inage-ku, Chiba 263-8522

(Received January 17, 2001)

The structures of diiodosamarium(II) complexes with amide compounds have been investigated basing on single crystal X-ray structural analyses. The reaction of $[SmI_2(thf)_2]$ with 2 equivalents of tetramethylurea (TMU) gave $[SmI_2(thf)_2(tmu)_2]$ (**1**). The three different kinds of ligands in **1** attach to the samarium atom in a trans orientation. $[SmI_2(thf)_2]$ reacted with 4 equivalents of 1,3-dimethyl-2-imidazolidione (DMI) to afford $[SmI_2(dmi)_4]$ (**2**), forming a typical hexa-coordinated octahedral structure. Diiodosamarium complex containing four *N*,*N*-dimethylacetamide (DMA) ligands $[SmI_2(dma)_4]$ (**3**) was prepared by treatment of $[SmI_2(thf)_2]$ with 4 equivalents of DMA. The reaction of $[SmI_2(thf)_2]$ with 6 equivalents of 1,3-dimethyl-3,4,5,6-tetrahydro-2-(1*H*)-pyrimidinone (dimethylpropyleneurea (DMPU)) gave $[Sm(dmpu)_6]I_2$ (**4**) quantitatively. This complex experiences a unique coordination fashion, in which six DMPU ligands coordinate to the samarium atom to overlap each other. $[SmI_2(dmpu)_3(thf)]$ (**5**) was isolated from the reaction of $[SmI_2(thf)_2]$ with 2 equivalents of DMPU. The reducing ability of these complexes was evaluated by reactions with benzylacetone or 9-haloanthracene. The structural analyses and reactivity studies of these complexes indicate that DMPU and DMA ligands are the most effective among the amide compounds to enhance the reducing ability of samarium diiodide.

After the pioneering work of Kagan and coworkers in 1977,[1] diiodosamarium(II) (SmI_2)-mediated organic reactions have been extensively investigated. This reagent has become one of the most important and useful one-electron reductants in synthetic organic chemistry.[2] It is well known that the addition of hexamethylphosphoric triamide (HMPA) to a solution of SmI_2 in tetrahydrofuran (THF) dramatically increases the reducing ability of divalent samarium species.[3] The molecular structures of HMPA coordinated diiodosamarium complexes, $SmI_2(hmpa)_4$[4] and $[Sm(hmpa)_6]I_2$, have also been determined by X-ray analyses,[5] and the structural information has become an important guide for the utilization of HMPA. Although the HMPA ligand reveals a prominent effect, one is reluctant to use it owing to its suspected carcinogenicity.[6] Recently, some urea derivatives and amide compounds, which are strong electron-donating ligands like HMPA, have been employed as alternative additives.[7–9] The effect of these amide complexes for the reduction enhancement of SmI_2 has been observed in many reactions, but the structure-reactivity relationships of the SmI_2 complexes generated in situ have not yet been elucidated.[10]

We consider that the characterization of the molecular structures of the diiodosamarium complexes with these additives and the evaluation of their reactivities are indispensable for further development of samarium diiodide-promoted organic reactions. In this paper, we report the X-ray structural analyses of diiodosamarium complexes bearing amide compounds such as tetramethylurea (TMU), 1,3-dimethyl-2-imidazolidinone (DMI), *N*,*N*-dimethylacetamide (DMA), and 1,3-dimethyl-3,4,5,6-tetrahydro-2-(1*H*)-pyrimidinone (dimethylpropyleneurea (DMPU)) as ligands. Furthermore, the coordination abilities of the amide compounds are discussed based on their coordination bond lengths; reactions of benzylacetone and 9-haloanthracene with these samarium complexes have been examined in order to elucidate their reducing abilities.

Experimental

General Methods. All reactions were carried out under argon atmosphere by using Schlenk techniques or under nitrogen atmosphere in an Mbraun glovebox. The nitrogen in the glovebox was constantly circulated through a copper/molecular sieves (4A) catalyst unit. The oxygen and moisture were constantly monitored by an O_2/H_2O Combi-Analyzer to ensure that both were always below 1 ppm. ^{1}H NMR spectra were recorded on JNM-LA400 (400.05 MHz for ^{1}H) spectrometer. Chemical shifts are reported in parts per million downfield from tetramethylsilane. Elemental analyses were carried out at The Institute of Physical and Chemical Research (RIKEN). THF, hexane, and toluene were distilled from sodium benzophenone ketyl, degassed by the freeze–thaw method (three times), and dried over fresh Na chips. Tetramethylurea, 1,3-dimethyl-2-imidazolidinone, 1,3-dimethyl-3,4,5,6-tetrahydro-2(1*H*)-pyrimidinone, and *N*,*N*-dimethylacetamide were purchased from Wako Pure Chemical Industries Co, dried by stirring with CaH_2 for 24 h, distilled under reduced pressure, and degassed by the freeze–thaw method (three times). Samarium metal was obtained from Nippon Yttrium Co. $[SmI_2(thf)_2]$ was prepared according to the literature.[11]

$[SmI_2(thf)_2(tmu)_2]$ (1). Addition of TMU (0.48 mL, 2 mmol) to a blue-green solution of $[SmI_2(thf)_2]$ (1.10 g, 2 mmol) in 20 mL of THF at room temperature caused an immediate color change to dark-purple. After 2 h, the solution was filtered through a frit and the solvent was removed under reduced pressure to give **1** as dark-purple powder (1.50 g, 96%). ^{1}H NMR (C_6D_6, 400 MHz, 25 °C): δ 0.70 (d, 3H, CH_3), 1.38 (s, 2H, CH_2), 3.58 (s, 2H, CH_2). (THF-

d_8, 400 MHz, 25 °C): δ 2.71 (t, 2H, CH_2), 3.10 (s, 3H, CH_3), 3.57 (d, 2H, CH_2), 5.40 (d, 3H, CH_3). IR (Nujol) 1584 (s), 1538 (s), 1412 (m), 1158 (m). 1037 (m), 912 (w), 878 (w), 766 (w), 748 (m), 722 (w), 670 (w), 566 cm^{-1} (m). Found: C, 27.54; H, 5.18; N, 7.46%. Calcd for $C_{18}H_{40}I_2N_4O_4Sm$: C, 27.69; H, 5.16; N, 7.18%. Slow cooling of the THF solution gave X-ray quality single crystals of $[SmI_2(thf)_2(tmu)_2\cdot(THF)_{0.67}]$, and its crystal solvent was easily removed in vacuo for 6 h to give $[SmI_2(thf)_2(tmu)_2]$.

$[SmI_2(dmi)_4]$ (2). DMI (0.86 mL, 8 mmol) was added to a solution of $[SmI_2(thf)_2]$ (1.10 g, 2 mmol) in 20 mL of THF at room temperature. After 2 h, the solvent was removed under reduced pressure, and the residue was washed with toluene to give **2** as a dark-purple powder (1.7 g, 99%). ^{1}H NMR (C_6D_6, 400 MHz, 25 °C) δ 2.40 (s, 2H, CH_2), 2.52 (s, 3H, CH_3). (THF-d_8, 400 MHz, 25 °C) δ 0.85 (s, 3H, CH_3), 1.25 (s, 3H, CH_3), 2.23 (s, 2H, CH_2), 2.41 (s, 2H, CH_2). IR (Nujol) 1660 (s), 1524 (s), 1408 (m), 1286 (s), 1245 (s), 1088 (w), 1041 (w), 967 (w), 778 (m), 758 cm^{-1} (w). Found: C, 28.08; H, 4.58; N, 12.76%. Calcd for $C_{20}H_{40}I_2N_8O_4Sm$: C, 27.91; H, 4.68; N, 13.02%. Single crystals for X-ray structural analysis were obtained by slow addition of DMI to a solution of SmI_2 in THF.

$[SmI_2(dma)_4]$ (3). DMA (7.43 mL, 80 mmol) was added to a solution of $[SmI_2(thf)_2]$ (11.0 g, 20 mmol) in 200 mL of THF at room temperature. After 2 h, the solvent was removed under reduced pressure to give **3** as a dark-purple powder (14.6 g, 97%). ^{1}H NMR (C_6D_6, 400 MHz, 25 °C) δ 1.66 (s, 3H, CH_3), 2.08 (s, 3H, CH_3), 2.61 (s, 3H, CH_3). Assignable peaks were not observed in THF-d_8 solution. IR (Nujol) 1618 (m), 1460 (s), 1380 (s), 1022 (m), 962 (w), 721 (m), 598 cm^{-1} (w). Found: C, 25.73; H, 4.84; N, 7.24%. Calcd for $C_{16}H_{36}I_2N_4O_4Sm$: C, 25.53; H, 4.82; N, 7.44%. Single crystals for X-ray structural analysis were obtained by slow addition of DMA to a solution of SmI_2 in THF.

$[Sm(dmpu)_6]I_2$ (4). DMPU (1.93 mL, 16 mmol) was added to a solution of $[SmI_2(thf)_2]$ (1.46 g, 2.67 mmol) in 20 mL of THF at room temperature. The pure solution was stirred at room temperature for 2 h. The solvent was removed under reduced pressure and the residue was washed with toluene to give a purple powder of **4** (3.0 g, 97%). ^{1}H NMR (C_6D_6, 400 MHz, 25 °C) δ 0.03 (s, 2H, CH_2), 1.12 (s, 3H, CH_3), 1.48 (s, 2H, CH_2). (THF-d_8, 400 MHz, 25 °C) δ 0.92 (t, 2H, CH_2), 1.14 (s, 2H, CH_2), 1.31 (s, 3H, CH_3), 2.01 (s, 3H, CH_3), 2.52 (s, 2H, CH_2). IR (Nujol) 1596 (s), 1548 (s), 1485 (m), 1417 (m), 1325 (m), 1253 (m), 1234 (w), 1065 (w), 943 (w), 893 (w), 746 (m), 712 cm^{-1} (w). Found: C, 36.95; H, 6.16; N, 13.92%. Calcd for $C_{36}H_{72}I_2N_{12}O_6Sm$: C, 36.86; H, 6.19; N, 14.33%. Slow addition of hexane to a concentrated THF solution of **4** gave single crystals for X-ray analysis.

$[SmI_2(dmpu)_3(thf)]$ (5). Method A: addition of DMPU (0.48 mL, 4 mmol) to a solution of $[SmI_2(thf)_2]$ (1.10 g, 2 mmol) in 20 mL of THF gave a dark-purple solution, which was stirred at room temperature for 2 h. The solution was concentrated and cooled to −20 °C. After 2 days, purple crystals were formed. Method B: the reaction of **4** (587 mg, 0.5 mmol) with $[SmI_2(thf)_2]$ (548 mg, 1 mmol) in 20 mL of THF also gave **5** (480 mg, 56% based on DMPU). In ^{1}H NMR analysis, no assignable peak was observed in THF-d_8 solution. Found: C, 30.52; H, 5.18; N, 9.57%. Calcd for $C_{22}H_{44}I_2N_6O_4Sm$: C, 30.70; H, 5.15; N, 9.76%. Single crystals for X-ray analysis were obtained by keeping a concentrated THF solution of **5** at −20 °C.

X-ray Crystallographic Analyses. The crystals were handled in a glovebox under a microscope (MZ6, Leica) which was mounted on the glovebox window, and were sealed in glass capillaries. Data collections were performed on a R-AXISII diffractometer with gaphite-monochromated Mo Kα radiation. A laser-stimulated fluorescence image plate was used as a two-dimensional area detector. Because of the instability of the crystals, rapid analysis was required. The distance between the crystal and the detector was 85 mm. Thus, 27 frames were recorded at intervals of 6° and each exposure lasted for 5 min (ca. 135 min for the total data collection). Molecular structures of complexes **1**, **2** and **4** were solved by direct methods using the programs SIR 92,[22] and that of complex **3** was solved by direct methods using the programs SAPI 91.[23] Full matrix less-squares refinements were carried out by minimizing the function $\Sigma\omega(|F_O| - |F_C|)^2$ where F_O and F_C were observed and calculated structure factors. The non-hydrogen atoms were refined anisotropically. Hydrogen atoms were included but not refined. The residual electron densities were of no chemical significance. Crystallographic data have been deposited at the CCDC, 12 Union Road, Cambridge CB2 1EZ, UK and copies can be obtained on request, free of charge, by quoting the publication citation and the deposition numbers 162183-162187. The data are also deposited as Document No. 74042 at the Office of the Editor of Bull. Chem. Soc. Jpn.

X-ray Structural Determination and Refinement for Complex 5. X-ray data collection was carried out as described above. The molecular structure was solved by direct methods using the programs SIR 92. The two iodide ions and one DMPU molecule are ordered, while two DMPU molecules and one THF molecule are disordered. Although the overall geometry of the complex has been established, location and refinement of all of the light atoms (C, N) of the disordered molecules were impossible. The best refinement of the model yielded $R = 11\%$. The space group is $P2_1/n$ with cell parameters of $a = 10.421(5)$ Å, $b = 15.980(10)$ Å, $c = 19.95(1)$ Å, $\beta = 99.01(5)°$, $V = 3281(2)$ Å^3, and $Z = 4$ for $D_{calcd} = 1.742$ g cm^{-3}.

General Procedure for Reactions of Benzylacetone with Diiodosamarium(II) Complexes (Table 6). Benzylacetone (0.15 mL, 1 mmol) was added to a solution (0.1 M, 2.2 mmol) of diiodosamarium(II) complex in THF at room temperature. The reaction mixture was treated with air and passed through a short column of silica gel using ethylacetate as the eluent. The solvent was removed on a rotary evaporator, and pinacol coupling product **6** and secondary alcohol **7** were isolated by preparative TLC ethylacetate/hexane (1:5) as the developing solvent.

Results and Discussion

Synthesis and Structure of $[SmI_2(thf)_2(tmu)_2]$ (1). We first attempted the isolation and structural characterization of a diiodosamarium(II) complex with TMU, which was used in SmI_2-promoted [3 + 2] cycloaddition reaction of carbonyl ylide.[7] The reaction of $[SmI_2(thf)_2]$ with 4 equivalents of TMU in THF gave **1**. Removal of the solvent gave a purple powder, and the resultant complex was recrystallized from THF to give dark-purple prisms. The molecular structure of complex **1** was determined by X-ray structural analysis. There are three molecules of the samarium complexes and a crystal solvent of two THF molecules in the crystallographic unit. Figure 1 shows the structure of one of the samarium complexes. The other complexes and the crystal solvent are omitted for clarity. The selected bond lengths and angles are listed in Table 1. Complex **1** contains two iodide ions, two TMU molecules, and two THF molecules. The ligand–Sm–ligand angles are in the range of 87°–93°, showing an ordinary octahedral structure. Three different kinds of ligands are located at the trans positions to

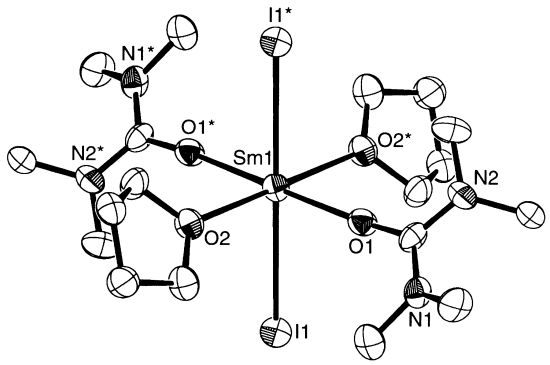

Fig. 1. Thermal ellipsoid plot of the structure of $[SmI_2(thf)_2(tmu)_2]$ (**1**).

Table 1. Selected Bond Lengths (Å) and Angles (deg) for $[SmI_2(thf)_2(tmu)_2]$ (**1**)

Sm(1)–I(1)	3.3169(9)	Sm(2)–I(2)	3.312(2)
Sm(3)–I(3)	3.3061(8)	Sm(1)–O(1)	2.458(8)
Sm(1)–O(2)	2.541(8)	Sm(2)–O(3)	2.436(7)
Sm(2)–O(4)	2.533(8)	Sm(3)–O(5)	2.444(7)
Sm(3)–O(6)	2.509(9)		
I(1)–Sm(1)–I(1*)	180	O(1)–Sm(1)–O(1)	87.6(2)
I(1)–Sm(1)–O(2)	87.4(2)	O(1)–Sm(1)–O(1*)	180
O(1)–Sm(1)–O(2)	93.8(3)	O(1)–Sm(1)–O(2*)	86.2(3)
O(2)–Sm(1)–O(2*)	180	Sm–O(1)–C(1)	171.7(8)

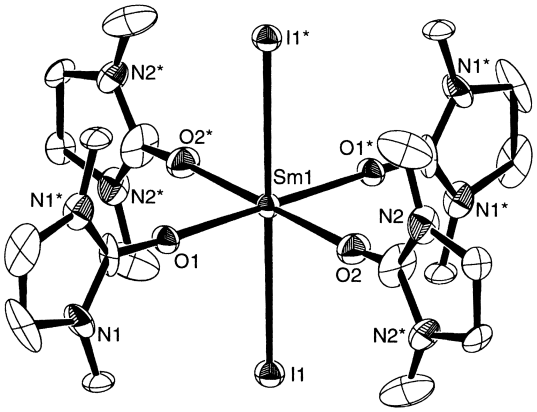

Fig. 2. Molecular structure of $[SmI_2(dmi)_4]$ (**2**).

Table 2. Selected Bond Lengths (Å) and Angles (deg) for $[SmI_2(dmi)_4]$ (**2**)

Sm(1)–I(1)	3.3578(9)	Sm(1)–O(1)	2.473(8)
Sm(1)–O(2)	2.59(1)	Sm(2)–I(2)	3.3450(9)
Sm(2)–O(3)	2.455(9)	Sm(2)–O(4)	2.396(6)
I(1)–Sm(1)–I(1*)	180	I(1)–Sm(1)–O(1)	90
I(1)–Sm(1)–O(2)	90	O(1)–Sm(1)–O(1*)	180
O(1)–Sm(1)–O(2)	87.7(3)	O(1)–Sm(1)–O(2*)	92.3(3)
O(2)–Sm(1)–O(2*)	180	Sm(1)–O(1)–C(1)	174.9(8)
Sm(1)–O(2)–C(4)	172(1)		

each other. Bond angles of I–Sm–I, O(THF)–Sm–O(THF), and O(TMU)–Sm–O(TMU) are just 180°, for there is a symmetry center on the samarium atom. The bond length of Sm–O(TMU) (2.446(7) Å) is shorter than that of Sm–O(THF) 2.528(9) Å, indicating that TMU molecules coordinate to the samarium atom more strongly than THF molecules.

Although 4 equivalents of TMU were added to $[SmI_2(thf)_2]$, the isolated complex contained only two TMU molecules, and the reaction of $[SmI_2(thf)_2]$ with 2 equivalents of TMU gave complex **1** quantitatively. The treatment of $[SmI_2(thf)_2]$ with a large excess of TMU (10 and 60 equivalents) also afforded complex **1**. These results are clearly different from those of HMPA coordinated diiodosamarium complexes.[4,5] Four HMPA coordinated samarium complex $SmI_2(hmpa)_4$ was obtained by the reaction of $[SmI_2(thf)_2]$ with 4 equivalents of HMPA. Moreover, a diiodosamarium complex bearing six HMPA molecules $[Sm(hmpa)_6]I_2$ was also obtained by the reaction of $[SmI_2(thf)_2]$ with 10 equivalents of HMPA. These results suggest that the coordination ability of the TMU ligand is weaker than that of HMPA.

Synthesis and Structure of $[SmI_2(dmi)_4]$ (2). The reaction of $[SmI_2(thf)_2]$ with 4 equivalents of DMI gave **2** quantitatively. Single crystals were obtained by slow addition of DMI to SmI_2 solution in THF, because of the poor solubility of complex **2** in this solvent. Its molecular structure was determined by X-ray structural analysis, as illustrated in Figure 2. The selected bond lengths and angles are shown in Table 2. This complex contains four DMI ligands and two iodide ions to form a regular hexa-coordinated octahedral structure. There are two molecules in the crystallographic unit, and four different bond lengths of Sm–O(DMI) are observed. The average bond length is 2.48(1) Å; however, the difference between the shortest bond length and the longest bond length is significantly large (0.2 Å), though the reason for this difference is not clear. The ligand–Sm–ligand angles are almost 90°. It is noted that all DMI ligands coordinate to the samarium atom in regularly perpendicular directions to the equatorial plane formed by four oxygen atoms of the DMI ligands. There is a mirror plane in the equatorial plane; therefore, the DMI ligands are divided into two equal parts crystallographically. $[SmI_2(thf)_2]$ was reacted with DMI by changing the molar equivalent of the ligand. It was found that $[SmI_2(dmi)_4]$ was always produced even through 10 equivalents of DMI was added.

Synthesis and Structure of $[SmI_2(dma)_4]$ (3). Inanaga et al. have investigated the selective reduction of α,β-unsaturated esters and amides with SmI_2.[9] The use of some additives such as dimethylformamide (DMF), DMA, TMU, *N*,*N*,*N*′,*N*′-tetramethylethylenediamine (TMEDA), and *N*,*N*,*N*′,*N*′-tetramethylpropylenediamine (TMPDA) promote effectively this conjugate reduction; DMA is the most effective ligand among these amides and amines. Therefore, we tried to isolate the DMA-coordinated diiodosamarium complex. The reaction of $[SmI_2(thf)_2]$ with 4 equivalents of DMA gave a dark-blue solution. Single crystals were obtained by slow addition of DMA to a SmI_2 solution in THF due to the poor solubility of the complex **3**. The crystal structure of $[SmI_2(dma)_4]$ (**3**) was determined by X-ray structural analysis. The ORTEP drawing of it is shown in Figure 3. The selected bond lengths and angles are summarized in Table 3. The central samarium atom is coordinated by the two iodide anions and the four DMA ligands to form a distorted octahedral structure. The four DMA ligands in the equatorial plane form a unique coordination

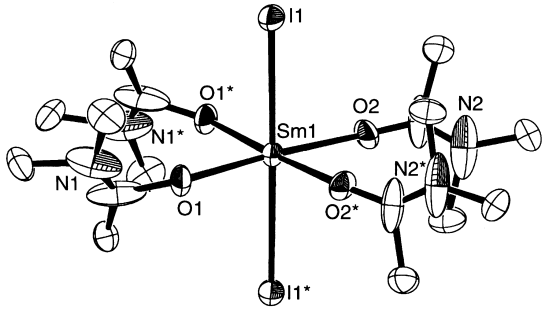

Fig. 3. ORTEP drawing of $[SmI_2(dma)_4]$ (**3**).

Table 3. Selected Bond Lengths (Å) and Angles (deg) for $[SmI_2(dma)_4]$ (**3**)

Sm(1)–I(1)	3.309(1)	Sm(1)–O(1)	2.45(1)
Sm(1)–O(1)	2.449(9)		
I(1)–Sm(1)–I(1*)	179.11(4)	I(1)–Sm(1)–O(1)	91.5(3)
I(1)–Sm(1)–O(2)	90.8(3)	O(1)–Sm(1)–O(1*)	85.1(5)
O(1)–Sm(1)–O(2)	177.4(4)	Sm(1)–O(1)–C(1)	138(1)
Sm(1)–O(2)–C(5)	143(1)		

fashion.

Synthesis and Structure of $[Sm(dmpu)_6]I_2$ (4). DMPU, a well-known and less toxic alternative to HMPA, has been employed as an additive in SmI_2-promoted organic reactions.[8] In order to isolate and clarify the molecular structure of DMPU ligand-coordinated diiodosamarium complex, $[SmI_2(thf)_2]$ was allowed to react with 4 equivalents of DMPU. The isolated crystals were subjected to X-ray structural analyses. The molecular structure of the complex is depicted in Figure 4. Table 4 shows the selected bond lengths and angles. There are two molecules in the unit cell, and the central samarium atom is hexacoordinated by six DMPU molecules. This complex has high symmetry; therefore, six DMPU ligands are crystallographically equivalent. The two iodide ions do not coordinate to the samarium atom, thus making the complex dicationic. To the best of our knowledge, dicationic divalent samarium complexes are very rare, and only a few complexes such as $[Sm(hmpa)_6]I_2$, $[Sm(thf)_7]^{2+}[Zn_4(\mu\text{-}SePh)_6(SePh)_4]^{2-}$[9,12] and $[Sm(dime)_3][Co(CO)_4]_2$ {dime = $(MeOCH_2CH_2)_2O$} are known.[13] The coordination number of the complex **4** is six, as in complexes **1**, **2**, and **3**; however, the coordination geometry of the central samarium atom is not octahedral but has a distorted trigonal antiprism structure. The large deviation in the ligand–Sm–ligand angle (O1–Sm–O1*) (76°) from 90° supports this coordination geometry. A samarium complex bearing six DMPU ligands could be isolated, but the corresponding complexes were not obtained when TMU, DMI, and DMA were used as the ligand. These facts suggest that coordination ability of DMPU is stronger than those of the other amide ligands. It is noteworthy that all DMPU ligands coordinate to the samarium atom while overlapping each other. The average bond angle of Sm–O–C (carbonyl carbon) (152°) is considerably different from that of complex **1** (171°) and complex **2** (175°), implying that some interaction exists between the upper ligands and lower ligands. However, the atomic distance between C1 and C19 (3.54(1) Å) is slightly longer than the sum of the van der Waals radii (ca. 3.0 Å), indicating that there is no intramolecular ligand interaction in the complex.

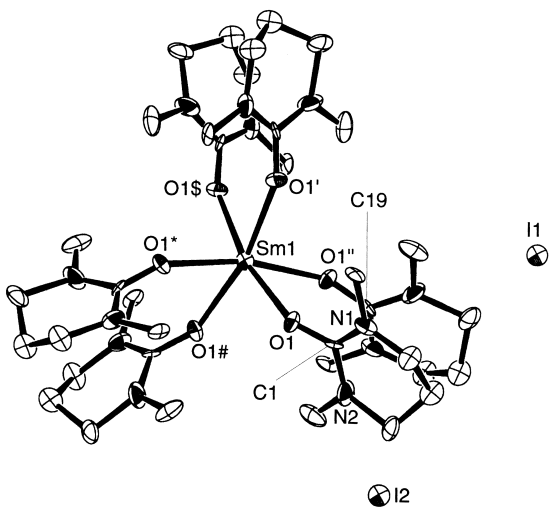

Fig. 4. Molecular structure of $[Sm(dmpu)_6]I_2$ (**4**).

Table 4. Selected Bond Lengths (Å) and Angles (deg) for $[SmI_2(dmpu)_6]I_2$ (**4**)

Sm(1)–O(1)	2.475(7)	Sm(2)–O(2)	2.488(9)
O(1)–Sm(1)–O(1″)	76.7(3)	O(1)–Sm(1)–O(1′)	94.6(2)
O(1)–Sm(1)–O(1$)	167.2(3)	O(1)–Sm(1)–O(1*)	94.6(2)
Sm(1)–O(1)–C(1)	151.1(7)		

A packing diagram for **4** indicates that $[Sm(dmpu)_6]I_2$ units of the backside position themselves so as to minimize the space between the front side units and the backside units (Figure 5). It is noted that the closest intermolecular contact between the methyl carbon of adjacent molecules (3.35(1) Å) is significantly less than the sum of the corresponding van der Waals radii (ca. 4.0 Å).

Synthesis and Structure of $[SmI_2(dmpu)_3(thf)]$ (5). The reaction of $[SmI_2(thf)_2]$ with 2 equivalents of DMPU provided a new diiodosamarium complex with DMPU ligands. The molecular structure of this complex **5** was determined and is shown in Figure 6. The crystallographic data reveal that three

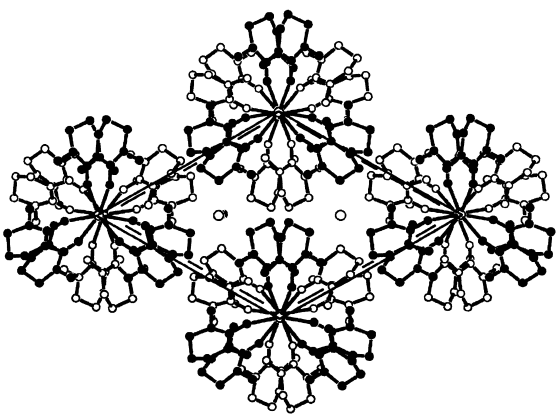

Fig. 5. Packing diagram of complex **4** looking down the "*c*" axis. Molecules indicated in black are front units and molecules indicated in white are back units.

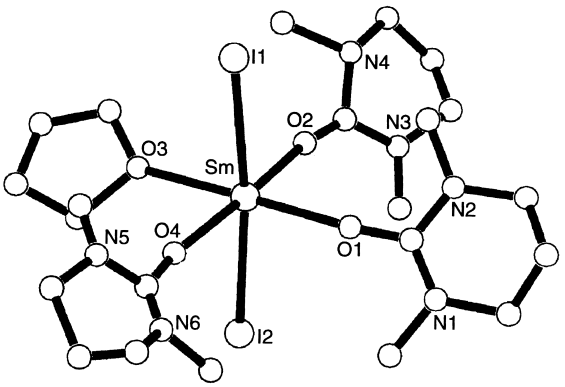

Fig. 6. Ball and stick plot of $[SmI_2(dmpu)_3(thf)]$ (**5**).

DMPU ligands, one THF molecule, and two iodide ions coordinate to the samarium atom to form a six-coordinated neutral complex, whereas **4** forms a dicationic complex. This complex was also obtained by the reaction of **4** with 2 equivalents of $[SmI_2(thf)_2]$, clearly indicating that ligand redistribution occurred in the reaction. Unfortunately, further discussion of bond distances and angles was hampered due to the limited quality of the crystallographic data.

Coordination Bond Lengths. In order to estimate the Sm^{III}/Sm^{II} reduction potential of complexes **1**, **2**, **3**, and **4**, the coordination bonds were compared with other divalent diiodosamarium complexes (Table 5). The bond distances between the samarium ion and the oxygen atoms of the amide compounds Sm–O(TMU) (av. 2.446(8) Å) in **1**, Sm–O(DMI) (av 2.48(1) Å) in **2**, Sm–O(DMA) (av 2.465(9) Å) in **3**, and Sm–O(DMPU) (av 2.482(9) Å) in **4** are much shorter than those of the corresponding coordination bonds of the divalent samarium complexes bearing oxygen donor ligands; e.g. Sm–O(DME) av 2.618(5) Å and Sm–O(THF) 2.530(5) Å in $[SmI_2(dme)_2(thf)]$,[14] Sm–O(DME) av 2.641(4) Å and Sm–O(THF) 2.571(4) Å in $[SmI_2(dme)(thf)_3]$,[14] Sm–O(diglyme) av 2.699(4) Å in $[SmI_2\{O(CH_2CH_2OMe)_2\}_2]$,[15] Sm–O(DME) av 2.67(1) Å in $[SmI_2(dme)_3]$[16] and Sm–O(THF) av 2.592(6) Å and Sm–O(DME) av 2.685(8) Å in $[Sm_2\{N(SiMe_3)_2\}(dme)_2(thf)_2(\mu\text{-}I)_2]$,[17] and they are almost the same or slightly shorter than those between the samarium atom and the oxygen atoms of HMPA (av 2.500(6) Å) in $SmI_2(hmpa)_4$ and (av 2.53(1) Å) in $[Sm(hmpa)_6]I_2$. These results clearly indicate that these amide compounds are strong donor ligands. Elongation of the Sm–I bonds was observed due to the strong coordination of amide ligands. The bond distances between the samarium ion and the iodide ion Sm–I (av 3.312(1) Å) in complex **1**, (av 3.3514(9) Å) in complex **2**, and 3.310(1) Å in complex **3** are slightly shorter than that of $SmI_2(hmpa)_4$ (3.390(2) Å), but they are longer than those of other diiodosamarium complexes such as $SmI_2(dme)_2(thf)$ 3.246(1) Å, $SmI_2(dme)(thf)_3$ av 3.233(1) Å, $[Sm(\mu\text{-}I)(NCCMe_3)_2]_\infty$ 3.260(1) Å and 3.225(1) Å,[15] *trans*-$[SmI_2\{O(CH_2CH_2OMe)_2\}_2]$ 3.265(1) Å,[15] *cis*-$[SmI_2\{O(CH_2CH_2OMe)_2\}_2]$ 3.332(1) Å and 3.333(1) Å,[18] $[Sm_2\{N(SiMe_3)_2\}(dme)_2(thf)_2(\mu\text{-}I)_2]$ av 3.3486(9) Å (bridge),[17] $[Sm_2I_2(\mu\text{-}I)(N\text{-Meim})_6]$ (*N*-Meim = *N*-methylimidazole) 3.237(1) Å (terminal), and av 3.294(1) Å (bridge).[19]

Table 5. Sm–I and Sm–O Bond Distances (Å) for Various Samarium Diiodide Complexes

	Bond distances, Å		
	Sm–I	Sm–O	Sm–O(THF)
$SmI_2(tmu)_2(thf)_2$[a)]	3.312(1)	2.446(8)	2.528(9)
$SmI_2(dmi)_4$[a)]	3.3514(9)	2.48(1)	
$SmI_2(dma)_4$[a)]	3.310(1)	2.449(9)	
$[Sm(dmpu)_6]I_2$		2.484(9)	
$SmI_2(hmpa)_4$	3.390(2)	2.500(6)	
$SmI_2(dme)_2(thf)$	3.246(1)	2.530(5)	
$SmI_2(dme)(thf)_3$	3.233(1)	2.571(4)	
trans-SmI_2 $[O(CH_2CH_2OMe)_2]_2$	3.265(1)	2.699(4)	

a) These bond distances are average data of Table 1–4.

In general, the coordination numbers of divalent samarium atoms are 7–9. In this case, it is noteworthy that the coordination numbers of all diiodosamarium complexes bearing amide ligands are six. The bond angles of O–C–N (Sm–O(THF)–C (**1**) 128.5°, O(TMU)–C–N (**1**) 119°, O(DMI)–C–N (**2**) 124.2°, O(DMA)–C–N (**3**) 102°, O(DMPU)–C–N (**4**) 124.9°, O(DMPU)–C–N (**5**) 123°) suggest that these amide ligands are relatively bulky, and therefore the coordination numbers of these complexes are comparatively small.

Reactions of Various SmI_2 Complexes with Benzylacetone. The isolated complexes were dissolved in THF-d_8 or benzene-d_6 and their NMR spectra were measured. It is noted that no peaks based on free amide ligands were observed. These results suggest that the molecular structures of the complexes in solution resemble those of the crystal system. Therefore, we considered that the reactivity of the complexes in solution can be correlated to their crystal structures. Based on this idea, we evaluated their reducing ability using benzylacetone as a representative carbonyl compound (Scheme 1). The reactions of the samarium(II) complexes with benzylacetone were carried out under the same reaction conditions. The obtained results are summarized in Table 6. SmI_2 itself required about 6 h to complete the reaction (entry 1). The reactivity of the complex **1** was nearly equal to that of SmI_2 itself, but the major product was **6** (entry 2). The reaction of SmI_2 with 10 equivalents of TMU also afforded the complex **1**. Therefore, these facts suggest that the reactivity of SmI_2 in the presence of 10 equivalents of TMU resembles that of complex **1**. In practice, however, this reductant revealed lowering of the reactivity and decreased selectivity of product **6** (entry 3). Flowers et al. reported that the oxidation potential of SmI_2 reached maximum when 60 equivalents of TMU was added.[21] In this reaction, SmI_2 with 60 equivalents of TMU showed low reactivity, and the major product was secondary alcohol **7** (entry 4). It was thought that excess TMU ligands in situ inhibited the reactivity and production of pinacol-coupling product **6**. The reactivity of the complex **2** was rather inferior to that of SmI_2 itself

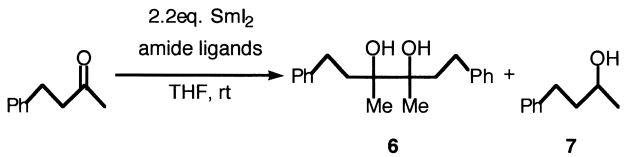

Scheme 1.

Table 6. Reactions of SmI_2 Complexes with Benzylacetone

Entry	Reductant	Time	Yield/% Conversion (**6**:**7**)[b]
1	$SmI_2(thf)_2$[a]	6 h	92 (34:66)
2	$SmI_2(tmu)_2$[a]	2 h	88 (82:18)
3	SmI_2 + 10 equiv TMU	2 h	75 (74:26)
4	SmI_2 + 60 equiv TMU	110 h	79 (19:81)
5	SmI_2 + 2 equiv DMI	2 h	73 (79:21)
6	$SmI_2(dmi)_4$[a]	18 h	76 (32:68)
7	SmI_2 + 10 equiv DMI	48 h	47 (0:100)
8	SmI_2 + 2 equiv DMA	30 min	100 (93:7)
9	$SmI_2(dma)_4$[a]	5 min	100 (93:7)
10	SmI_2 + 6 equiv DMA	15 min	97 (92:8)
11	SmI_2 + 10 equiv DMA	2 h	70 (66:34)
12	SmI_2 + 1 equiv DMPU	15 min	82 (81:19)
13	SmI_2 + 2 equiv DMPU	5 min	100 (85:15)
14	SmI_2 + 3 equiv DMPU	15 min	100 (81:19)
15	SmI_2 + 4 equiv DMPU	15 min	100 (84:16)
16	SmI_2 + 5 equiv DMPU	2 h	71 (75:25)
17	$[Sm(dmpu)_6]I_2$[a]	2 h	61 (41:59)
18	SmI_2 + 30 equiv DMPU	110 h	64 (13:87)
19	$SmI_2(hmpa)_4$[a]	15 min	100 (42:58)
20	SmI_2 + 6 equiv HMPA	1 h	79 (14:86)

a) Isolated complex was disolved in THF, and the solution (0.1 M) was used for the reaction.
b) Determined by ^{1}H NMR.

(entry 6). On the other hand, the complex **3** demonstrated high reactivity, and the reaction was completed within 5 minutes (entry 9). To our surprise, reactivities of the SmI_2/DMPU systems greatly depended on the amounts of DMPU (entry 12–18). One equivalent of DMPU per SmI_2 was not sufficient to show high reactivity (entry 12). The additions of 2–4 equivalents of DMPU to SmI_2 revealed high reactivities (entry 13–15). The reactivity of the complex **4** was clearly different from that of SmI_2 with 2 equivalents of DMPU (entry 17). The oxidation potential of SmI_2 reached a maximum when 30 equivalents of DMPU added,[21] but it showed a low reactivity (entry 18). Hou and Wakatsuki have carried out the X-ray structural analysis of $[Sm(hmpa)_6]I_2$ and clearly demonstrated that six HMPA molecules could coordinate to a samarium atom. On the other hand, Flowers et al. have recently investigated in detail the structure of a samarium diiodide-HMPA complex in THF solution by UV-vis spectroscopy, isothermal titration (ITC), and vapor pressure osmometry (VPO).[20] They concluded that a four HMPA coordinated samarium complex was stable but a six HMPA coordinated complex was thermodynamically unstable under standard reaction conditions. In the case of SmI_2/HMPA system, no prominent reactivity change was observed because a major complex is $[SmI_2(hmpa)_4]$ in THF solution even in the presence of excess HMPA. In contrast with HMPA, the great reactivity change in SmI_2/DMPU system reveals that more than five DMPU ligands can coordinate to a samarium atom.

Reduction of 9-Chloroanthracene. It was reported that the addition of HMPA to SmI_2 dramatically promoted the reduction of organic halides.[3] In order to evaluate their reducing abilities, the reactions of 9-haloanthracene with diiodosamarium complexes bearing amide ligands were carried out at room temperature. The amide ligands were effective in the reduction

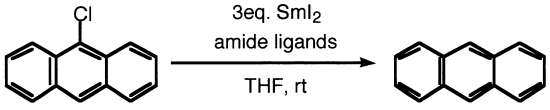

Scheme 2.

Table 7. Reactions of SmI_2 Complexes with 9-Chloroanthracene

Entry	Reductant	Time	Yield/%[a]
1	$SmI_2(thf)_2$	24 h	no reaction
2	$SmI_2(tmu)_2$	24 h	5
3	$SmI_2(dmi)_4$	24 h	2
4	$SmI_2(dma)_4$	4 h	94
5	$[Sm(dmpu)_6]I_2$	4 h	34
6	SmI_2 + 4 equiv DMPU	4 h	96
7	SmI_2 + 2 equiv DMPU	4 h	65
8	$SmI_2(hmpa)_4$	1 min	$>$ 99

a) Determined by ^{1}H NMR.

of 9-bromoanthracene, but this reaction was not good for comparison of ligand effects. Therefore, 9-chloroanthracene was used as substrate because its reactivity is lower than 9-bromoanthracene (Scheme 2). The results are shown in Table 7. No anthracene was obtained in the reaction of SmI_2 itself (entry 1), and complexes **1** and **2** afforded trace amounts of anthracene (entry 2 and 3). The complex **3** showed moderate reactivity to afford anthracene in high yield (entry 4). The reactivities of SmI_2/DMPU systems depended on the amounts of DMPU as observed in the reactions of benzylacetone (entry 5–7); 4 equivalents of DMPU per SmI_2 revealed the highest reactivity (entry 6). $[SmI_2(hmpa)_4]$ exhibited high reactivity to give anthracene quantitatively (entry 8). The reactivities of SmI_2 with amide ligand are a little lower than that of the SmI_2/HMPA system. However, enough reactivity could be obtained when using 4 equivalents of DMPU or DMA to SmI_2.

Recently, the effect of oxygen donor ligands on the oxidation potential of SmI_2 was examined by voltammetric analysis.[21] The reduction potential (Sm^{III}/Sm^{II}) of SmI_2/DMPU system (-2.21 V) was lower than that of the SmI_2/TMU system (-2.04 V). These facts also suggest that DMPU is a stronger electron-donating ligand than TMU ligand.

Diiodosamarium(II) complexes bearing amide compounds have been isolated and structurally characterized by X-ray diffraction analysis (Table 8). The coordination number of these complexes is six, which is smaller than those (7–9) of the usual divalent samarium complexes, indicating that amide compounds are strong electron-donating and bulky ligands. DMPU and DMA ligands are shown to be most effective to enhance the reducing power of SmI_2, but the reactivities of these complexes are slightly lower than that of $[SmI_2(hmpa)_4]$. Furthermore, it is found that the reactivities of SmI_2 with amide ligands, in particular DMPU, greatly depend on the amounts of amide ligand per SmI_2.

This work was suported by "Research for the Future" Program, the Japan Society for the Promotion of Science.

Table 8. Crystallographic Data for $SmI_2(thf)_2(tmu)_2$ (**1**), $SmI_2(dmi)_4$ (**2**), $SmI_2(dma)_4$ (**3**), and $[Sm(dmpu)_6]I_2$ (**4**)

	1	**2**	**3**	**4**
Formula	$C_{62}H_{136}I_6N_{12}O_{14}Sm_3$	$C_{20}H_{40}I_2N_8O_4Sm$	$C_{16}H_{36}I_2N_4O_4Sm$	$C_{36}H_{72}I_2N_{12}O_6Sm$
Fw	2486.46	860.80	752.69	1173.25
Crystal system	triclinic	monoclinic	tetragonal	trigonal
Color of crystal	purple	blue	purple	purple
Space group	*P*1	*C*2/*m*	$P4_32_12$	*P*321
a, Å	13.442(10)	14.265(7)	10.011(4)	12.965(2)
b, Å	13.409(6)	15.147(6)		
c, Å	13.402(5)	14.25(2)	26.132(7)	16.333(7)
α, deg	99.44(3)			
β, deg	99.45(3)	89.59(7)		
γ, deg	98.96(3)			
V, Å^3	2308(2)	3080(4)	2619(1)	2377(1)
Z	1	4	4	2
T/K	173	173	173	110
D_{calcd}, g cm^{-3}	1.788	1.856	1.909	1.639
μ(Mo $K\alpha$)/cm^{-1}	39.50	39.53	46.30	25.90
No. of obsd rflns	6783 ($I > 2.0\sigma(I)$)	1893 ($I > 2.0\sigma(I)$)	1199 ($I > 2.0\sigma(I)$)	1495 ($I > 2.0\sigma(I)$)
$R(R_w)$[a)]	0.085(0.136)	0.075(0.127)	0.054(0.080)	0.082(0.119)
GOF	2.24	2.07	1.87	1.70

a) $R = \Sigma||F_O| - |F_C||/\Sigma|F_O|$, $R_w = [\Sigma w(|F_O| - |F_C|)^2/\Sigma wF_O^2]^{1/2}$.

References

1 a) J. L. Namy, P. Girard, and H. B. Kagan, *New. J. Chem.*, **1**, 5 (1977). b) P. Girard, J. L. Namy, and H. B. Kagan, *J. Am. Chem. Soc.*, **102**, 2693 (1980). c) J. L. Namy, P. Girard, and H. B. Kagan, *New. J. Chem.*, **5**, 479 (1981).

2 For representative reviews, see: a) H. B. Kagan and J. L. Namy, *Tetrahedron*, **42**, 6573 (1986). b) G. A. Molander, "Comprehensive Organic Synthesis," ed by B. M. Trost, Pergamon, Oxford (1991), Vol. 1, p. 251. c) H. B. Kagan, M. Sasaki, and J. Collin, *Pure Appl. Chem.*, **60**, 1725 (1988). d) G. A. Molander, *Chem. Rev.*, **92**, 29 (1992). e) G. A. Molander and C. R. Harris, *Chem. Rev.*, **92**, 307 (1996). f) T. Imamoto, "Lanthanides in Organic Synthesis," ed by A. R. Katrizky, O. Meth-Corn, C. W. Rees, Academic Press: London, 1994, 21. g) H. B. Kagan, J. L. Namy, "Topics in Organometallic Chemistry Volume 2, Lanthanide: Chemistry and Use in Organic Synthesis," ed by S. Kobayashi, Springer, Germany (1999).

3 a) K. Otsubo, J. Inanaga, and M. Yamaguchi, *Tetrahedron Lett.*, **27**, 5763 (1986). b) J. Inanaga, M. Ishigawa, and M. Yamaguchi, *Chem. Lett.*, **1987**, 1485. c) K. Otsubo, J. Inanaga, and M. Yamaguchi, *Chem. Lett.*, **1987**, 1487. d) Y. Handa, J. Inanaga, and M. Yamaguchi, *J. Chem. Soc., Chem. Commun.*, **1989**, 298. e) O. Ujikawa, J. Inanaga, and M. Yamaguchi, *Tetrahedron Lett.*, **30**, 2837 (1989). f) J. Inanaga, O. Ujikawa, and M. Yamaguchi, *Tetrahedron Lett.*, **32**, 1737 (1991). g) J. Inanaga, Y. Handa, T. Tabuchi, K. Otsubo, M. Yamaguchi, and T. Hanamoto, *Tetrahedron Lett.*, **32**, 6557 (1991).

4 Z. Hou and Y. Wakatsuki, *J. Chem. Soc., Chem. Commun.*, **1994**, 1205.

5 Z. Hou, Y. Zhang, and Y. Wakatsuki, *Bull. Chem. Soc. Jpn.*, **70**, 149 (1997).

6 T. Mukhopadhyay and D. Seebach, *Helv. Chim. Acta*, **65**, 385 (1982).

7 Use of TMU in SmI_2 reaction: M. Hojo, H. Aihara, and A. Hosomi, *J. Am. Chem. Soc.*, **118**, 3533 (1996).

8 Uses of DMPU in SmI_2 reactions: a) T. L. Fevig, R. C. Elliott, and D. P. Curran, *J. Am. Chem. Soc.*, **110**, 5064 (1988). b) L. Crombie and L. J. Rainbow, *Tetrahedron Lett.*, **29**, 6517 (1988). c) S. M. Bennett and D. Larouche, *Synlett*, **1991**, 805. d) D. P. Curran and R. L. Wollin, *Synlett*, **1991**, 317. e) I. Fleming and S. K. Ghosh, *J. Chem. Soc., Chem. Commun.*, **1992**, 1775. f) E. Hasegawa and D. P. Curran, *J. Org. Chem.*, **58**, 5008 (1993). g) G. A. Molander and S. R. Shakya, *J. Org. Chem.*, **59**, 3445 (1994). h) E. Vedejs and S. Lin, *J. Org. Chem.*, **59**, 1602 (1994). i) C. Goulaouic-Dubois, A. Guggisberg, and M. Hesse, *J. Org. Chem.*, **60**, 5969 (1995). j) Z. Zhou, D. Larouches, and S. M. Bennett, *Tetrahedron*, **51**, 11623 (1995). k) R. A. Batey, J. D. Haring, and W. B. Motherwell, *Tetrahedron*, **52**, 11421 (1996).

9 Use of DMA in SmI_2 reaction: J. Inanaga, S. Sakai, Y. Handa, M. Yamaguchi, and Y. Yokoyama, *Chem. Lett.*, **1991**, 2117.

10 R. S. Miller, J. M. Sealy, M. Shabangi, M. L. Kuhlman, J. R. Fuchs, and R. A. Flowers, II, *J. Am. Chem. Soc.*, **122**, 7718 (2000).

11 W. J. Evans, J. W. Grate, H. W. Choi, I. Bloom, W. J. Hunter, and J. L. Atwood, *J. Am. Chem. Soc.*, **107**, 941 (1985).

12 M. Berardini, T. J. Emge, and J. G. Brennan, *Inorg. Chem.*, **34**, 5327 (1995).

13 J. P. White III, H. Deng, E. P. Boyd, J. Gallucci, and S. G. Shore, *Inorg. Chem.*, **33**, 1685 (1994).

14 W. J. Evans, T. S. Gummersheimer, and J. W. Ziller, *J. Am. Chem. Soc.*, **117**, 8999 (1995).

15 V. R. Chebolu, R. Whittle, and A. Sen, *Inorg. Chem.*, **24**, 3082 (1985).

16 M. Håkansson, M. Vestergren, B. Gustafsson, and G. Hilmersson, *Angew. Chem., Int. Ed.*, **38**, 2199 (1999).

17 W. J. Evans, D. K. Drummond, H. Zhang, and J. L. Atwood, *Inorg. Chem.*, **27**, 575 (1988).

18 A. Sen, V. Chebolu, and A. L. Rheingold, *Inorg. Chem.*, **26**, 1821 (1987).

19 W. J. Evans, G. W. Rabe, and J. W. Ziller, *Inorg. Chem.*, **33**, 3072 (1994).

20 J. B. Shotwell, J. M. Sealy, and R. A. Flowers, II, *J. Org. Chem.*, **64**, 5251 (1999).

21 a) M. Shabangi, J. M. Sealy, J. R. Fuchs, and R. A. Flowers, II, *Tetrahedron Lett.*, **39**, 4429 (1998). b) M. Shabangi, M. L. Kuhlman, R. A. Flowers, II, *Org. Lett.*, **1**, 2133 (1999).

22 A. Altomare, M. C. Burla, M. Camalli, M. Cascarano, C. Giacovazzo, A. Guagliardi, and G. Polidori, "SIR92, Program for the Solution of Crystal Structure," 1994.

23 F. Hai-Fu, "SAPI91, Structure Analysis Program with Intelligent Control," Rigaku Corporation, Tokyo, Japan (1991).